CDF note 11072

Measurement of the Top-Quark Mass in the $t\bar{t}$ Dilepton Channel Using the Full CDF Run II Data Set

The CDF Collaboration
URL http://www-cdf.fnal.gov
(Dated: March 2, 2015)

We present a measurement of the top-quark mass in $t\bar{t}$ dilepton events. We use the full dataset collected by CDF during the Fermilab Tevatron Run II at the center-of-mass energy $\sqrt{s} = 1.96$ TeV, and corresponding to an integrated luminosity of 9.1 fb^{-1}. A special observable is exploited for an optimal reduction of the dominant systematic uncertainty associated to the jet-energy scale. The distribution of this observable in the candidate events is compared to simulated templates of $t\bar{t}$ dilepton signal and background. Using a maximum-likelihood fit, we measure a top-quark mass value of $171.46 \pm 1.91(\text{stat}) \pm 2.51(\text{syst})GeV/c^2$.

I. INTRODUCTION

The top-quark mass ($M_{\rm top}$) is one of the fundamental parameters of the Standard Model (SM). Precise measurements of the top-quark mass are important for a check of the self-consistency of the SM by global electroweak fits [1].

In the CDF Run II we study proton-antiproton collisions at a center-of-mass energy 1.96 TeV. Top quarks are mostly produced in pairs ($t\bar{t}$) from quark-antiquark annihilations (∼85%) or from gluon-gluon fusion. Both top quarks decay almost exclusively as $t \to Wb$. The channels of $t(\bar{t})$-decay are classified according to the decay modes of the W boson. To improve the precision the top-quark mass should be measured independently in all decay channels. In the present analysis, we consider the events in the dilepton final state, which is defined by the presence of two charged leptons (electrons or muons), two or more jets, and a large imbalance in the total transverse momentum from the two neutrinos associated with the charged leptons ("$t\bar{t}$ dilepton events").

This paper reports a measurement of the top-quark mass in the dilepton channel with full CDF Run II data set corresponding to 9.1 fb^{-1} of integrated luminosity. This analysis updates the last CDF result [2] with additional data collected at the end of Run II and corresponding to integrated luminosity of about 3 fb^{-1}.

For the recent $M_{\rm top}$ measurements in the dilepton channel, the statistical uncertainty is less important than the systematic one, which is dominated by the uncertainty on the jet-energy scale (JES). Measurements in the other final states reduce the JES systematic uncertainty by imposing a dijet mass constraint for jets originated from hadronic W boson decay, which permits a precise calibration of the calorimeter JES (*"in-situ"* calibration). In contrast to the other final states, dilepton events do not feature jet pairs originating from W boson decay and accordingly can't yield a dijet mass signature which permits a precise calibration of jet energies. This fact requires to direct the efforts to searches of new possibilities for reduction of systematics due to JES uncertainty. In our analysis we optimize the total uncertainty of measurement. This method applied to the increased data sample results in reducing a total uncertainty by 14% with reference to the previous measurement [2].

II. DATA SAMPLE & EVENT SELECTION

The data were collected with an inclusive lepton trigger that require an electron with $\rm E_T > 18$ GeV (or a muon with $\rm P_T > 18$ GeV/c) in the central region of the detector. The analyzed event sample was obtained with selection criteria developed for the $t\bar{t}$ cross section measurement in the dilepton channel [4]. Also we have introduced additional cuts in our analysis to improve modeling and to reduce background.

Below we just list the basic selection requirements and refer for details to the above-cited note. We select events with two high-$\rm E_T$ leptons of opposite charge, one of which must be isolated. Here we require $\rm E_T > 20$ GeV for electrons or $\rm P_T > 20$ GeV/c for muons. Missing transverse energy must be $\not\!\!E_{\rm T} > 25$ GeV indicating the presence of neutrino. A supplementary requirement is applied to e^+e^- and $\mu^+\mu^-$ events when the invariant mass of the dilepton system is in the interval of ± 15 GeV/c^2 from the mass of the Z boson. For these events, we require a $\not\!\!E_{\rm T}$ significance [3] of > 4 GeV$^{1/2}$. Events in which $\not\!\!E_{\rm T}$ originates from mis-measurement of the leptons or jets typically have small azimuthal angle $\Delta\phi'$ between the $\not\!\!E_{\rm T}$ vector and the direction of the mis-measured object. To reject this instrumental background, we increase the $\not\!\!E_{\rm T}$-requirement to $\not\!\!E_{\rm T} > 50$ GeV for events where $\Delta\phi' < 20^\circ$ relative to some jet axis or lepton. Two (or more) jets with corrected $\rm E_T > 15$ GeV and $|\eta| < 2.5$ are also required. The transverse energy sum, H_T, has to be more than 200 GeV, and the dilepton invariant mass has to be larger than 5 GeV.

Our additional cuts are presented below. We require the minimal distance in the η-ϕ space between any lepton and any jet in event, $\Delta R_{lj} = \sqrt{\Delta\eta_{lj}^2 + \Delta\phi_{lj}^2}$, has to be more than 0.2. This cut reduces significantly the background of events with fake leptons. We reject events with the reconstructed mass $M_t^{\rm reco}$ (see section III B) more than 250 GeV. We introduce this requirement because simulation shows that the tail of the $M_t^{\rm reco}$ distribution contains mainly background events. We also tighten the cut on the dilepton invariant mass. We require the dilepton invariant mass to be larger than 10 GeV. This is done in order to reject events from processes which we do not model.

In total we have 520 dilepton candidates after these selection requirements. The same cuts are applied to the Monte Carlo events generated for signal or background processes. The sensitivity of our measurement to the top-quark mass can be improved by analyzing separately events with beauty-flavored (b-tagged) jets. We divide the event sample into two mutually exclusive sub-samples: b-tagged and non-tagged ones. The first sub-sample contains events which have at least one tight SecVtx b-tagged jet [5]. The non-tagged sub-sample contains events which have no tight SecVtx b-tagged jets and events for which the b-tagging algorithm cannot be applied. Table I gives the summary of expected contributions and observed events for the b-tagged and

CDF Run II Preliminary (9.1 fb^{-1})

$t\bar{t}$ **dilepton sample**		
Source	Tagged events	0 tag events
WW	0.57 ± 0.15	16.4 ± 3.6
WZ	0.12 ± 0.03	5.2 ± 1.0
ZZ	0.20 ± 0.06	3.0 ± 0.5
DY/Z	4.4 ± 0.4	51.2 ± 8.0
Fakes	8.6 ± 2.7	21.4 ± 6.2
Total background	13.9 ± 2.8	97.2 ± 14.5
$t\bar{t}$ ($\sigma = 7.4$ pb)	227.2 ± 16.2	173.2 ± 13.3
Total SM expectation	241.1 ± 16.4	270.3 ± 26.4
Observed	230	290

TABLE I: Summary table of expected contributions and observed events in SecVtx b-tagged and non-tagged dilepton data samples.

non-tagged samples.

III. CALCULATING THE VARIABLE FOR TOP QUARK MASS MEASUREMENT

A. "Hybrid" variable's method

To measure the top-quark mass we perform the template analysis using a variable sensitive to the top-quark mass. For analysis we have built a variable that is expected to achieve the smallest uncertainty of the measurement. To determine this variable, we start from two initial observables. The first variable is the reconstructed mass $M_t^{\rm reco}$. We calculate it using a kinematic fit of dilepton events (see III B). We take the reconstructed mass for analysis as the variable that is the most sensitive to the top-quark mass. In contrast to $M_t^{\rm reco}$ our second one is the most sensitive to the top-quark mass variable that we can build without using information about jet energies. This variable is insensitive to jet energy scale (JES) but is not as sensitive to the top-quark mass as $M_t^{\rm reco}$. We denote it here as "alternative" mass, $M_{lb}^{\rm alt}$. Details of $M_{lb}^{\rm alt}$ calculation can be found in Section III C. We define the "hybrid" variable for template analysis using the weighted sum of these two variables. In this note we will denote the introduced variable as $M^{\rm hyb}$:

$$M^{\rm hyb} = w \cdot M_t^{\rm reco} + (1 - w) \cdot M_{lb}^{\rm alt}, \tag{1}$$

where w is some parameter. By varying w from 1 to 0, $M^{\rm hyb}$ varies from $M_t^{\rm reco}$ to $M_{lb}^{\rm alt}$. The statistical and systematic uncertainties of the measurement depend on the choice of the w parameter. We choose the value of w with which we expect to obtain the result with the smallest uncertainty. We will discuss the choice of optimal value of w in Section III D.

We choose the "hybrid" variable's method as alternative of the best linear unbiased estimator (BLUE) [6]. In contrast to BLUE we don't need to combine correlated results because we operate within the template method framework.

B. Calculating the reconstructed mass

The method implemented in this analysis for reconstructing the top-quark mass event by event is called the "Neutrino ϕ Weighting Method". This method was previously used for top-quark mass measurement on the lepton+track sample [7].

Due to the existence of two neutrinos we have a non-constrained kinematics. The number of independent variables is one more than the number of kinematic constrains: a total number of 24 unknown (b, $\overline{b}$, l^-, l^+, ν and $\overline{\nu}$ 4-momenta) and only 23 equations to constrain the kinematics (measured 3-momenta for two b-jets and two leptons, assumed known mass for 6 final particles, used two transverse components of calorimeter missing energy, constrained invariant mass for two W and assumed equal constrained mass of top and antitop quarks).

In order to constrain the kinematics, the scanning over the space of possibilities for the azimuthal angles of neutrinos ($\phi_{\nu_1}, \phi_{\nu_2}$) is used. A top-quark mass is reconstructed by minimizing a chi-squared function (χ^2) in the dilepton $t\bar{t}$ event hypothesis. The χ^2 has two terms:

$$\chi^2 = \chi^2_{reso} + \chi^2_{constr} \tag{2}$$

The first term takes into account the detector uncertainties, whereas the second one constrains the parameters to the known physical quantities given their uncertainties. The first term is as follows:

$$\chi^2_{reso} = \sum_{l=1}^{2} \frac{(P_T^l - \tilde{P_T^l})^2}{{\sigma^l_{P_T}}^2} - 2\sum_{j=1}^{2} \ln(\mathscr{P}_{tf}(\tilde{P_T^j}|P_T^j)) + \sum_{i=x,y} \frac{(UE^i - \tilde{UE^i})^2}{{\sigma_{UE}}^2} \tag{3}$$

With the use of the tilda ($\sim$) we specify the parameters of the minimization procedure, whereas variables without tilda represent the measured values. $\mathscr{P}_{tf}$ are the transfer functions between b-quark and jets: they express the probability of measuring a jet transverse momentum P_T^j from a given b-quark with transverse momentum $\tilde{P_T^j}$. The sum in the first term is over the two leptons in the event; the second sum loops over the two highest-E_T (leading) jets, which are assumed to originate from the b quarks. After candidate events are selected, leading jets momenta are further corrected for multiple interactions, underlying event, and out-of-cone energy loss.

The third sum runs over the transverse components of the unclustered energy (UE^x, UE^y), which is defined as the sum of the energy vectors from the towers not already associated with leptons or any leading jets.

The uncertainties (σ_{P_T}) on the lepton P_T used for electrons (e) and muons (μ) are calculated as [7]:

$$\frac{\sigma^e_{P_T}}{P^e_T} = \sqrt{\frac{0.135^2}{P^e_T[\mathrm{GeV}/c]} + 0.02^2} \tag{4}$$

$$\frac{\sigma^\mu_{P_T}}{P^\mu_T} = 0.0011 \cdot P^\mu_T[\mathrm{GeV}/c] \tag{5}$$

Uncertainty in the transverse components of the unclustered energy, σ_{UE}, is defined from phenomenological formula $\sigma_{UE}[\mathrm{GeV/c}] = 0.4\sqrt{\sum E_T^{\mathrm{uncl}}[\mathrm{GeV/c}]}$ [8], where E_T^{uncl} is the scalar sum of the transverse energy excluding two leptons and two leading jets.

The second term in Eq. 2, χ^2_{constr}, constrains the parameters of the minimization procedure through the invariant masses of the lepton-neutrino and of the lepton-neutrino-leading jet systems. This term is as follows:

$$\begin{aligned}\chi^2_{constr} = &-2\ln(\mathscr{P}_{BW}(m^{l_1,\nu_1}_{inv}|M_W,\Gamma_{M_W})) - 2\ln(\mathscr{P}_{BW}(m^{l_2,\nu_2}_{inv}|M_W,\Gamma_{M_W})) \\ &-2\ln(\mathscr{P}_{BW}(m^{l_1,\nu_1,j_1}_{inv}|\tilde{M}_t,\Gamma_{\tilde{M}_t})) - 2\ln(\mathscr{P}_{BW}(m^{l_2,\nu_2,j_2}_{inv}|\tilde{M}_t,\Gamma_{\tilde{M}_t}))\end{aligned} \tag{6}$$

$\tilde{M}_t$ is the parameter giving the reconstructed top-quark mass. $\mathscr{P}_{BW}(m_{inv};\ m,\Gamma) \equiv \frac{\Gamma^2 \cdot m^2}{(m^2_{inv} - m^2)^2 + m^2\Gamma^2}$ indicates the relativistic Breit-Wigner distribution function, which expresses the probability that an unstable particle of mass m and decay width Γ decays into a system of particles with invariant mass m_{inv}. We use the PDG values for M_W and Γ_{M_W}. For the top width we use the function

$$\Gamma_{M_t} = \frac{G_F}{8\sqrt{2}\pi} M_t^3 (1 - \frac{M_W^2}{M_t^2})^2 (1 + 2\frac{M_W^2}{M_t^2}) \tag{7}$$

according to Ref. [9].

The longitudinal components of the neutrino momenta are free parameters of the minimization procedure, while the transverse components are related to $\overrightarrow{\not{E}_{\mathrm{T}}}$ and to the assumed $(\phi_{\nu_1}, \phi_{\nu_2})$ as follows:

$$\begin{cases} P^{\nu_1}_x \equiv P^{\nu_1}_T \cdot \cos(\phi_{\nu_1}) = \frac{\not{E}_{\mathrm{T}T_x} \cdot \sin(\phi_{\nu_2}) - \not{E}_{\mathrm{T}T_y} \cdot \cos(\phi_{\nu_2})}{\sin(\phi_{\nu_2} - \phi_{\nu_1})} \cdot \cos(\phi_{\nu_1}) \\ P^{\nu_1}_y \equiv P^{\nu_1}_T \cdot \sin(\phi_{\nu_1}) = \frac{\not{E}_{\mathrm{T}T_x} \cdot \sin(\phi_{\nu_2}) - \not{E}_{\mathrm{T}T_y} \cdot \cos(\phi_{\nu_2})}{\sin(\phi_{\nu_2} - \phi_{\nu_1})} \cdot \sin(\phi_{\nu_1}) \\ P^{\nu_2}_x \equiv P^{\nu_2}_T \cdot \cos(\phi_{\nu_2}) = \frac{\not{E}_{\mathrm{T}T_x} \cdot \sin(\phi_{\nu_1}) - \not{E}_{\mathrm{T}T_y} \cdot \cos(\phi_{\nu_1})}{\sin(\phi_{\nu_1} - \phi_{\nu_2})} \cdot \cos(\phi_{\nu_2}) \\ P^{\nu_2}_y \equiv P^{\nu_2}_T \cdot \sin(\phi_{\nu_2}) = \frac{\not{E}_{\mathrm{T}T_x} \cdot \sin(\phi_{\nu_1}) - \not{E}_{\mathrm{T}T_y} \cdot \cos(\phi_{\nu_1})}{\sin(\phi_{\nu_1} - \phi_{\nu_2})} \cdot \sin(\phi_{\nu_2}) \end{cases} \tag{8}$$

The minimization procedure described above must be performed for all the allowed values of ϕ_{ν_1}, ϕ_{ν_2} in the $(0, 2\pi) \times (0, 2\pi)$ region. Based on simulation, we choose a ϕ_{ν_1}, ϕ_{ν_2} grid of 24×24 values as inputs for the

minimization procedure. In building the grid we avoid the singular points at $\phi_{\nu_1} = \phi_{\nu_2} + k \cdot \pi$, where k is integer. Note from Eq. 8 that performing the transformation $\phi_\nu \to \phi_\nu + \pi$ leaves P_x^ν and P_y^ν unchanged, but reverses the sign of P_T^ν. We exclude unphysical solutions ($P_T^{\nu_1} < 0$ and/or $P_T^{\nu_2} < 0$) and choose the solution which leads to positive transverse momenta for both neutrinos. This decreases the number of grid points to 12×12. At each point 8 solutions can exist, because of the two-fold ambiguity in the longitudinal momentum for each neutrino and of the ambiguity on the lepton-jet association. Therefore, for each event, we perform 1152 minimizations, each of which returns a value of M_{ijk}^{reco} and χ^2_{ijk} ($i, j = 1, \ldots, 12$; $k = 1, \ldots, 8$). We define $\chi'^2_{ij} = \chi^2_{ij} + 4 \cdot \ln(\Gamma_{M_t})$, which is obtained by using Eq. 6 where $\mathscr{P}_{BW}$ is substituted with $\mathscr{P}'_{BW} \sim \frac{\Gamma \cdot m^2}{(m^2_{inv} - m^2)^2 + m^2\Gamma^2}$, and select the lowest χ'^2 solution for each point of the $(\phi_{\nu_1}, \phi_{\nu_2})$ grid, thereby reducing the number of obtained masses to 144. Each mass is weighted. Based on simulation, we choose the next weights:

$$w_{ij} \;=\; \frac{e^{-\chi'^2_{ij}/2}}{\sum_{i=1}^{12}\sum_{j=1}^{12} e^{-\chi'^2_{ij}/2}}. \tag{9}$$

A mass distribution is built and the most probable value is identified (MPV). Masses below a threshold of 30% the MPV bin content are discarded, and the remaining ones are averaged to compute the reconstructed top-quark mass for the event $M_t^{\rm reco}$.

C. Defining $M_{lb}^{\rm alt}$ such as to be insensitive to the jet energy scale

In order to define $M_{lb}^{\rm alt}$ as a variable insensitive to JES we must avoid making use of jet energies. Observable, denoted as "alternative" mass ($M_{lb}^{\rm alt}$), is defined according to the following formula:

$$M_{lb}^{\rm alt} \;=\; c^2 \sqrt{\frac{\langle l_1, b_1\rangle \cdot \langle l_2, b_2\rangle}{E_{b_1} \cdot E_{b_2}}}, \tag{10}$$

where l_1 and l_2 are the four-momenta of leptons, b_1 and b_2 are the four-momenta of the two highest-E_T ("leading") jets, which are defined as for massless particles, with energies E_{b_1} and E_{b_2}. The quantity $\langle l,b\rangle$ indicates the scalar product of the l and b four-vectors. Although the jet energies E_{b_1} and E_{b_2} appear in Eq. 10, $M_{lb}^{\rm alt}$ does not depend on their values but depends only on the jet directions. We use the same index (1 or 2) to indicate a lepton and a jet which are assumed to originate from the decay of the same top quark. The use of the two leading jets in Eq. 10 is justified because, according to simulation, in about 78% of the selected $t\bar{t}$ events the two leading jets originate from the hadronization of the two b-quarks in the $t\bar{t}$ decay. To choose between the two possible pairings of leptons to jets, the proximity of track directions of leptons and jets is examined. We specify the track direction of the leptons and b-jets through the unit vector $\boldsymbol{c} = (c_x, c_y, c_z)$, where c_x, c_y, and c_z are the direction cosines of their momenta. The pairing with the largest sum of scalar products $\langle \boldsymbol{c}_{l_1}, \boldsymbol{c}_{b_1}\rangle + \langle \boldsymbol{c}_{l_2}, \boldsymbol{c}_{b_2}\rangle$ is chosen. The indexes l_1 and b_1 (l_2 and b_2) correspond to the lepton and b-jet in the first (second) pair. From simulation, we estimate that this lepton-to-jet pairing criterion selects the right pairing in about 60% of cases.

D. Optimizing the measurement

We scan the [0,1] range of the w parameter in Eq. (1) in steps of 0.05 in order to find the optimal value for our measurement. For every point of the scan, we define the mass fit procedure using the signal and background templates for $M^{\rm hyb}$ and evaluate the statistical and systematic uncertainties. This procedure is absolutely the same as described in the next Sections of this note. We build the signal and background templates for $M^{\rm hyb}$, define likelihood and perform pseudo-experiments (PE's). We check that mass and uncertainties found in the PE's are correct. We define the expected statistical uncertainty as the average statistical uncertainty in PE's with input top-quark mass of 172.5 GeV/c^2. We evaluate the JES systematic uncertainty by applying shifts in JES. The systematic uncertainties from sources other than JES were studied for a few values of w: 0, 0.3, 0.5, 0.7 and 1. The total systematic uncertainty generated by sources other than JES ("non-JES uncertainty") is calculated as the sum in quadrature of these uncertainties. To estimate the non-JES systematic uncertainty for any value of w we use the cubic spline interpolations. The obtained values of the expected statistical uncertainty, and of JES, non-JES, expected total uncertainties are shown as a function of w in Fig. 1. The expected total uncertainty is estimated as the sum in quadrature of the obtained uncertainties.

Although $M_{lb}^{\rm alt}$ does not depend explicitly on JES, the $M_{\rm top}$ measurement using only $M_{lb}^{\rm alt}$ (points with $w = 0$ in Fig. 1) is still affected by uncertainty in JES because JES has an impact on event selection. When varying

JES according to its uncertainty, the change in the event sample accepted by the cuts on variables that depend on jet energies generates the change in the $M_{lb}^{\rm alt}$ distribution that affects the $M_{\rm top}$ measurement. We find that by shifting JES, opposite systematic shifts are induced in the results of the $M_{\rm top}$ measurements using $M_{lb}^{\rm alt}$ and $M_t^{\rm reco}$ (points with $w = 0$ and with $w = 1$ in Fig. 1). This testifies that two effects generated by the uncertainty in JES, i.e. the impact on the variable being used and the effect induced via the event selection, shift the $M_{\rm top}$ measurement in opposite directions. Having this in mind, the dependence on w of the JES systematic uncertainty can be understood as follows. While at large w values the first effect dominates, we have a compensation on the interval of the w-values from 0.10 to 0.15, and below approximately $w = 0.10$ the second effect starts to dominate.

For this analysis, we chose to use the likelihood fit corresponding to $w = 0.6$. This choice was motivated by the observation that around $w = 0.6$ the expected total uncertainty has a wide minimum. We observe an 9% improvement in the total uncertanty in the case of $w = 0.6$ with respect to an analysis that uses only the reconstructed top-quark mass $M_t^{\rm reco}$ ($w = 1$).

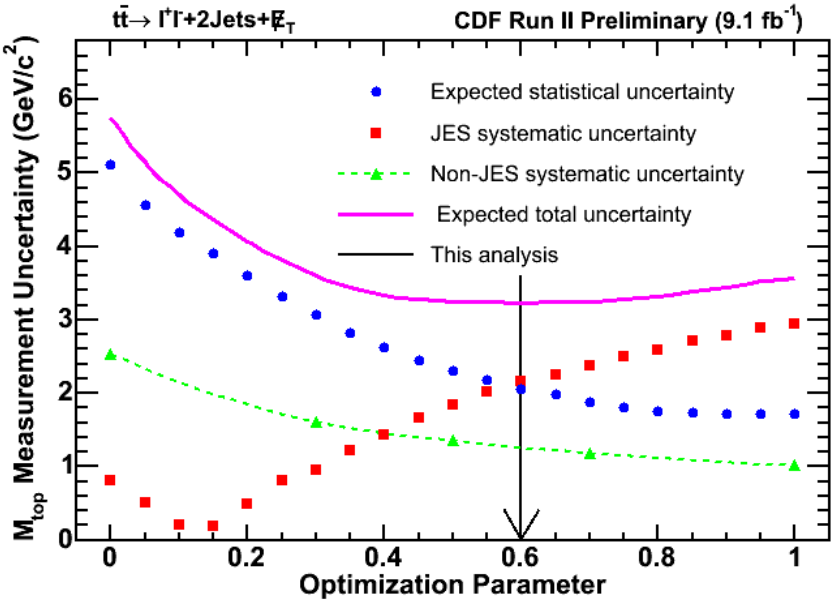

FIG. 1: Uncertainties in the measurement of $M_{\rm top}$ as a function of w (Eq. 1).

IV. TOP-QUARK MASS DETERMINATION

A. Templates

The selected data sample is a mixture of signal and background events. In order to extract the top-quark mass, the $M^{\rm hyb}$ distribution (see Eq. 1) in data is compared with probability density functions (p.d.f.'s) for signal and background by means of a likelihood fit. Signal templates are built separately for b-tagged and non-tagged events from $t\bar{t}$ samples generated for top-quark masses M_t in the range from 160 GeV/c^2 to 185 GeV/c^2 with 1 GeV/c^2 steps. The probability density functions (p.d.f.'s) of the signal, $P_s(M^{\rm hyb}|M_t)$, which express the probability of getting any $M^{\rm hyb}$ value in $t\bar{t}$ events with given M_t, are obtained as parameterizations of sets of corresponding templates. We parameterize the templates using a sum of two Landau and one Gaussian probability distribution functions. The parameters of these functions linearly depend on M_t. The background templates are built separately for b-tagged and non-tagged events by adding diboson, fakes, and Drell-Yan templates which are normalized to the expected rates reported in Table I. The background p.d.f.'s, $P_b(M^{\rm hyb})$, are obtained from a likelihood fit of the combined background templates, performed as the same way like for the signal templates, but without any parameter dependence on M_t.

B. Likelihood Form

The top-quark mass is extracted from the data sample by performing an unbinned likelihood fit. We define the likelihood function as product of independent likelihood functions obtained for b-tagged and non-tagged subsamples:

$$\mathscr{L}^{total} = \mathscr{L}^{tag} \cdot \mathscr{L}^{notag}. \tag{11}$$

The likelihood functions, $\mathscr{L}^{tag}$ and $\mathscr{L}^{notag}$, express the probability that a top mass distribution from data is described by a mixture of background events and dilepton $t\bar{t}$ events with an assumed top-quark mass. Inputs for the likelihood are the values of $M^{\rm hyb}$ from data events, the signal and background p.d.f.'s and the expected background. The background expectations are taken from Table I. The likelihoods, $\mathscr{L}^{tag}$ and $\mathscr{L}^{notag}$, have the same form:

$$\mathscr{L} = \mathscr{L}_{shape} \cdot \mathscr{L}_{backgr}; \tag{12}$$

where

$$\mathscr{L}_{shape} = \frac{e^{-(n_s+n_b)} \cdot (n_s+n_b)^N}{N!} \cdot \prod_{n=1}^{N} \frac{n_s \cdot P_s(M^{\rm hyb}|M_{top}) + n_b \cdot P_b(M^{\rm hyb})}{n_s+n_b}, \tag{13}$$

$$\mathscr{L}_{backgr} = \exp(\frac{-(n_b - n_b^{exp})^2}{2\sigma^2_{n_b^{exp}}}). \tag{14}$$

The shape likelihood term, $\mathscr{L}_{shape}$ (Eq. 13), expresses the probability of an event being signal with a top-quark mass of M_{top} or background. The signal (P_s) and background (P_b) probabilities are weighted according to the number of signal (n_s) and background (n_b) events, which are floated in the likelihood fit. In the fitting procedure, n_b is constrained to be Gaussian-distributed with mean value n_b^{exp} and standard deviation $\sigma_{n_b^{exp}}$, as shown by Eq. 14, while $(n_s + n_b)$ is the mean of a Poisson distribution of N selected events.

We perform the likelihood fit using the MINUIT [10] program. The fit returns a top-quark mass estimator (M_{top}^{fit}) and an estimated numbers of signal ($n_s^{tag\ fit}$ and $n_s^{notag\ fit}$) and background events ($n_b^{tag\ fit}$ and $n_b^{notag\ fit}$). M_{top}^{fit} returned by the likelihood fit is the mass corresponding to the minimum of the $[-\ln \mathscr{L}^{total}]$ function. Its statistical positive and negative uncertainties are the difference between M_{top}^{fit} and the mass values at $[-ln(\mathscr{L})]_{min} + 0.5$. The positive and negative statistical uncertainties (σ^+ and σ^-) are returned by MINOS [10]. The obtained result is presented with symmetrized statistical uncertainty: $\sigma = (\sigma^+ + |\sigma^-|)/2$.

C. Bias checks

We checked whether the fit with likelihood form (11) is able to return the correct mass. Checks are performed by running a large number of "Pseudo-experiments" (PE's) on simulated background and signal events where the true top-quark mass is known. Each PE consists of determining the number of signal (N_s^{PE}) and background (N_b^{PE}) events in the sample, drawing N_s^{PE} masses from a signal template and N_b^{PE} from the background template, and likelihood fitting, as described in Sec. IV B. A top-quark mass (M_t^{fit}) and its symmetrized statistical uncertainty are returned by the fit. Numbers of signal and background events are generated according to Poisson distributions with means given in Tables I. Performing for each $M_{\rm top}^{\rm inp}$ a number of PE's typically as large as 2500 we check that $M_t^{\rm fit}$ is an unbiased estimate of $M_{\rm top}$, and that its uncertainty is correctly estimated.

V. SYSTEMATIC UNCERTAINTIES

Since our method compares findings to expectations estimated from Monte Carlo simulations, uncertainties in our models used to generate events cause systematic uncertainties. We calculate the contribution to the systematics from each source of uncertainty. The generic procedure for estimating a systematic uncertainty is as follows. The parameters used for the generation of events are modified by $\pm$ 1 standard deviation in their uncertainties and new templates are built. PE's from the modified templates are performed using the same

p.d.f.'s as in the analysis. The difference between the median of the top-quark mass distribution from PE's and the nominal top-quark mass is used as the estimate of the systematic uncertainty.

The largest contribution comes from the uncertainty in the jet energy measurement, which includes uncertainties due to the following effects: non-uniformity in calorimeter response as a function of $|\eta|$, multiple $p\bar{p}$ collisions, hadronic jet energy scale, underlying events, and out-of-cone energy lost in the clustering procedure.

Difference between data and MC luminosity profile is accounted by rescaling the top-quark mass dependence on the number of interactions in the event by the difference in the number of interactions between data and MC.

The initial and final state radiation (IFSR) uncertainties are estimated using the Pythia Monte Carlo samples, in which the QCD parameters for parton shower evolution in the initial and final states are varied simultaneously. The amount of variation is based on the CDF studies of Drell-Yan data.

The uncertainty in reconstructing the top-quark mass due to the use of a particular parton distribution function (PDF) comes from three sources: PDF parametrization, PDF choice, and QCD scale (Λ_{QCD}).

The effect of using different $t\bar{t}$ Monte Carlo generators is checked by comparing the nominal PYTHIA with alternative HERWIG samples. Also, we estimate the systematics due to the NLO effects by the comparison of the PYTHIA and POWHEG generators.

In order to estimate the systematic uncertainty for the background composition, the expected rates of fakes, diboson, and Drell-Yan events are alternatively varied by plus or minus one standard deviation without changing the total number of expected background events. We also studied the effect from changing the shape of the main background contributors: Drell-Yan and "fakes".

The uncertainty for the b-jet scale due to the heavy quark fragmentation, semileptonic b-jet branching ratio, and b-jet calorimeter response is also taken into account. The effect of the fragmentation model on the top quark mass is evaluated by reweighting events according to two different fragmentation models, while effects of the uncertainties on the semileptonic b-jet branching ratio (BR) and b-jet energy calorimeter response are estimated by shifting the BR and the b-jet energy scale.

The effect on the top-quark mass from the uncertainty on lepton energy scale is studied by applying $\pm 1\%$ shifts to the lepton p_T.

The effect of color reconnection (CR) on our result is studied using the PYTHIA 6.4 MC generator, which includes CR effects.

The effect of the limited statistics of the employed Monte Carlo samples is evaluated by the bootstrap method.

Since PYTHIA is a leading-order MC generator the number of $t\bar{t}$ events from gluon fusion in PYTHIA samples is approximately 6% while the NLO expectation is $15\% \pm 5\%$. We take into account the uncertainty in the top-quark mass due to this effect.

Also the effect on the top-quark mass from the uncertainty in b-tagging modeling is studied.

The source of each systematic uncertainty is assumed to be uncorrelated to the other ones, so that the overall systematic error is obtained by adding in quadrature the individual uncertainties. The systematic uncertainties along with the total uncertainty are summarized in Table II. The total systematic uncertainty is estimated as 2.51 GeV/c^2.

VI. RESULTS

With $w = 0.6$, and allowing for statistical uncertainties only, the likelihood fit to the data sample provides $M_{\rm top} = 171.46 \pm 1.91$ GeV/c^2. The experimental top-quark mass distributions for b-tagged and non-tagged subsamples are shown in Figure 2. The fitted mass-dependent negative log-likelihood function from the likelihood fit to the dilepton data sample is presented in Figure 3. Also the post-fit plots for our initial variables ($M_t^{\rm reco}$ and $M_{lb}^{\rm alt}$) are presented in Figures 4 and 5.

In order to check that the measured statistical uncertainty is reasonable, a set of PE's is performed on simulated background and signal events with $M_t = 171$ GeV/c^2 (close to the central value of the constrained fit). We estimate that the probability for obtaining a precision better than that found in this experiment (p-value) is 39%. This value is obtained by comparing the measured statistical uncertainty with those expected from PE's.

CDF Run II Preliminary (9.1 fb^{-1})

$M_{\rm top}$ Measurement in the $t\bar{t}$ Dilepton Final State	
Source	Uncertainty (GeV/c^2)
Jet energy scale	2.17
NLO effects	0.67
Monte Carlo generators	0.50
Lepton energy scale	0.41
Background modeling	0.39
Initial and final state radiation	0.38
gg fraction	0.31
b-jet energy scale	0.30
Luminosity profile (pileup)	0.27
Color reconnection	0.24
MC sample size	0.20
Parton distribution functions	0.16
b-tagging	0.05
Total systematic uncertainty	2.51
Statistical uncertainty	1.91
Total	**3.15**

TABLE II: Summary of uncertainties on the top-quark mass measurement.

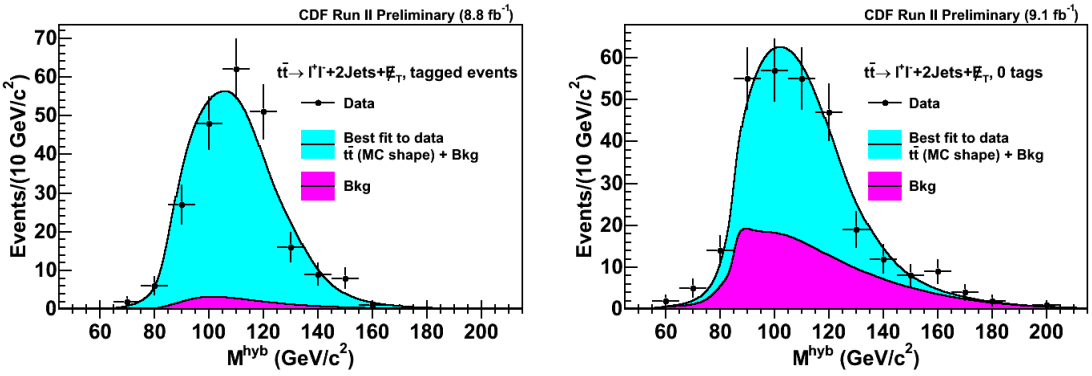

FIG. 2: Likelihood fit to the $t\bar{t}$ dilepton data sample. Background (purple) and signal+background (cyan) p.d.f.'s, normalized according to the numbers returned by the fitter, are superimposed to the top-quark mass distribution from data (points). Left and right plots are for b-tagged and non-tagged subsamples respectively.

VII. CONCLUSION

Using the full CDF Run II data set we measure on a $t\bar{t}$ dilepton sample a top-quark mass of

$$\begin{aligned} M_{\rm top} &= 171.46 \pm 1.91\ ({\rm stat}) \pm 2.51\ ({\rm syst})\ {\rm GeV}/c^2 \\ &\text{or} \\ M_{\rm top} &= 171.46 \pm 3.15\ {\rm GeV}/c^2. \end{aligned} \tag{15}$$

The measured value of $M_{\rm top}$ is compatible with the world average top-quark mass ($M_{\rm top} = 173.34 \pm 0.76$ GeV/c^2 [11]). This measurement updates the previous CDF result [2] obtained in the dilepton final state. The accuracy achieved is approximately 14% better than in the previous measurement.

Acknowledgments

We thank the Fermilab staff and the technical staffs of the participating institutions for their vital contributions. This work was supported by the U.S. Department of Energy and National Science Foundation; the Italian Istituto Nazionale di Fisica Nucleare; the Ministry of Education, Culture, Sports, Science and Technology of

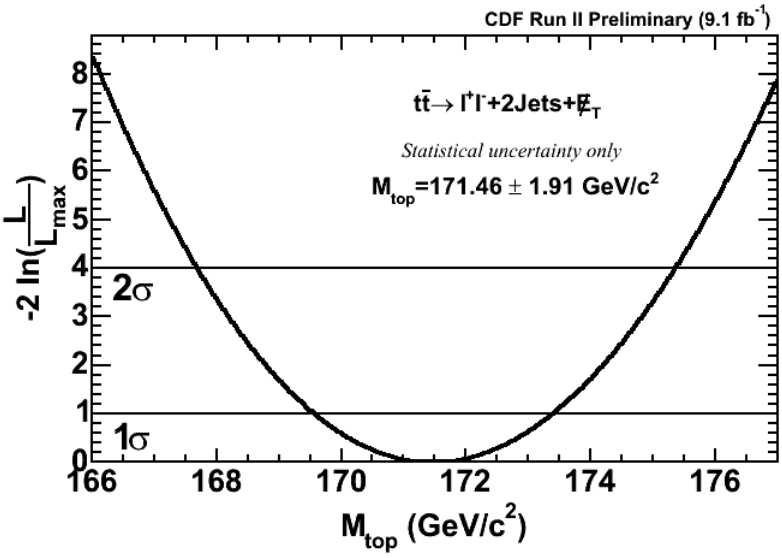

FIG. 3: Twice the fitted mass-dependent negative log-likelihood function from the likelihood fit to the $t\bar{t}$ dilepton data sample.

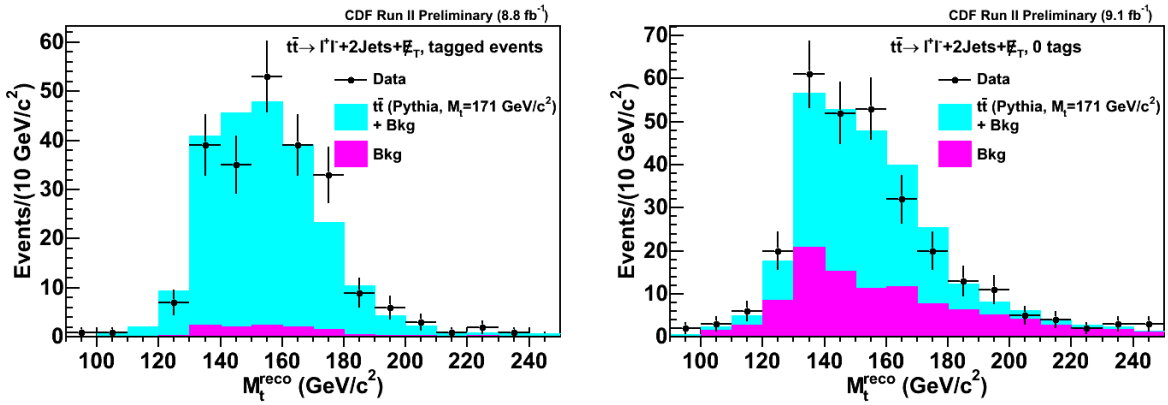

FIG. 4: Background (purple) and signal+background (cyan) templates for the reconstructed top-quark mass, normalized according to the numbers returned by the fitter, are superimposed to the reconstructed mass distribution from data (points). Left and right plot are for b-tagged and non-tagged subsamples respectively. The value 171 GeV/c^2 is assumed for the top-quark mass (close to the central value of the data fit).

Japan; the Natural Sciences and Engineering Research Council of Canada; the National Science Council of the Republic of China; the Swiss National Science Foundation; the A.P. Sloan Foundation; the Bundesministerium für Bildung und Forschung, Germany; the Korean World Class University Program, the National Research Foundation of Korea; the Science and Technology Facilities Council and the Royal Society, United Kingdom; the Russian Foundation for Basic Research; the Ministerio de Ciencia e Innovación, and Programa Consolider-Ingenio 2010, Spain; the Slovak R&D Agency; the Academy of Finland; the Australian Research Council (ARC); and the EU community Marie Curie Fellowship Contract No. 302103.

[1] M. Baak, M. Goebel, J. Haller, A. Hoecker, D. Kennedy, R. Kogler, K. Moenig, M. Schott, and J. Stelzer, Eur. Phys. J. C **72**, 2205 (2012).
[2] T. Aaltonen et al., The CDF Collaboration, Phys. Rev. D83, 111101 (2011); arXiv: 1105.0192;
[3] Variable named $\not\!\!E_T$ significance is defined as $\not\!\!E_T/\sqrt{E_T^{\rm sum}}$. The value of $E_T^{\rm sum}$ is calculated as the sum of transverse

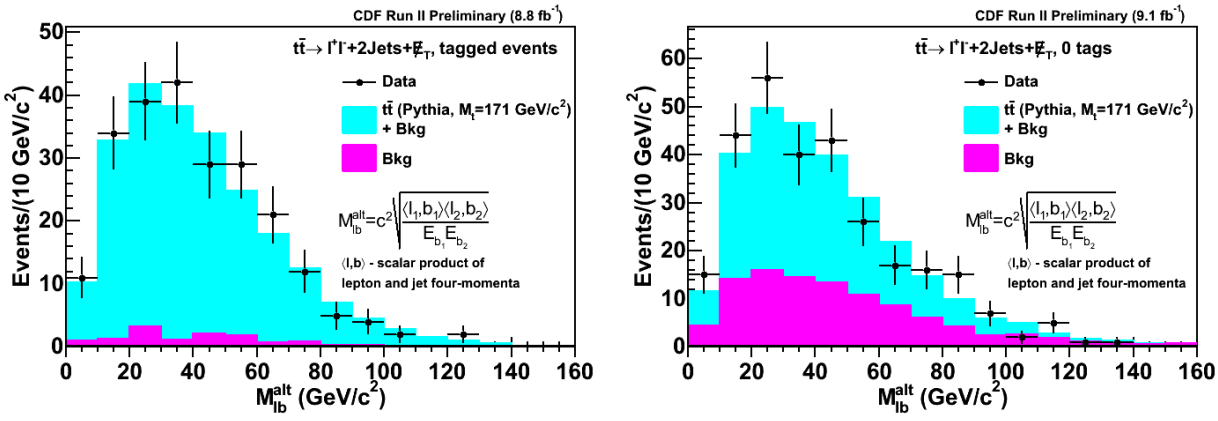

FIG. 5: Background (purple) and signal+background (cyan) templates for $M_{lb}^{\rm alt}$ variable, normalized according to the numbers returned by the fitter, are superimposed to the $M_{lb}^{\rm alt}$ variable distribution from data (points). Left and right plot are for b-tagged and non-tagged subsamples respectively. The value 171 GeV/c^2 is assumed for the top-quark mass (close to the central value of the data fit).

energies deposited in calorimeter towers and is corrected with the muon transverse momenta for events with identified muons and also corrected for various instrumental effects.
[4] T. Aaltonen et al., The CDF Collaboration, Phys. Rev. D 88, 091103 (2013);
[5] D. Acosta et al., The CDF Collaboration, Phys. Rev. D 71, 052003 (2005);
[6] L. Lyons, D. Gibaut, and P. Clifford, Nucl. Instrum. Meth. A270 (1988) 110, A. Valassi, Nucl. Instrum. Meth. A500 (2003) 391;
[7] T. Aaltonen et al., The CDF Collaboration, Phys. Rev. D 79, 072005 (2009);
[8] A. Abulencia et al., CDF Collaboration, Phys. Rev. D 73, 032003 (2006);
[9] M. Beneke et al., Top Quark Physics, arXiv:hep-ph/0003033;
[10] F. James, *MINUIT: Function Minimization and Error Analysis*, CERN Program Library, D506;
[11] G. Aad *et al.* (ATLAS, CDF, CMS, and D0 Collaborations), arXiv:1403.4427 [hep-ex].